J Sol-Gel Sci Technol (2014) 71:246–253
DOI 10.1007/s10971-014-3361-1

ORIGINAL PAPER

Hybrid organic–inorganic sol–gel coatings with interpenetrating network for corrosion protection of tinplate

Jian-Guo Liu · Liang Xu · Yong-Qin Fang

Received: 9 December 2013 / Accepted: 9 April 2014 / Published online: 24 April 2014

Abstract Novel hybrid organic–inorganic coatings with interpenetrating network were synthesized by the acid-catalyzed hydrolytic co-polycondensation of tetraethoxysilane and 3-metacryloxypropyltrimethoxysilane, followed by radical polymerization with methyl methacrylate and triallyl isocyanurate (TAIC). The hybrid coatings were characterized by Fourier transformed infrared spectroscopy, thermogravimetric analysis and scanning electron microscope, and their anti-corrosion behaviors were evaluated by potentiodynamic polarization, electrochemical impedance spectroscopy and salt spray test. The results indicated that the hybrid coatings exhibited excellent anti-corrosion ability by forming a physical barrier between metal and its external environment. Thermal stability of the hybrid coatings was increased after the addition of TAIC. Furthermore, hydrophobic properties of the hybrid coatings were examined by measuring the contact angles, and the change in wetting characteristics of the hybrid coatings was not obvious.

Keywords Hybrid coatings · Corrosion protection · Interpenetrating network · Tinplate · Salt spray test

J.-G. Liu · Y.-Q. Fang (✉)
Institute of Design and Research, ChangZhou University, Changzhou 213164, China
e-mail: f13506119729@126.com

L. Xu
Changzhou Institute of Advanced Materials, BUCT, Changzhou 213164, China

1 Introduction

Metal corrosion usually occurs after the chemical reactions between the metal surface and the environment, which leading to an irreversible disintegration of the material accompanied by the formation of oxides, hydroxides and salts. As a result, steel would lose its aesthetic appearance and structural integrity [1]. The most common corrosion prevention method is the chromium conversion coating [2], which forms insoluble trivalent chromium products by metal dissolution and precipitation of a passive layer of corrosion product. However, chromate conversion coatings are extremely poisonous to humans' health and generate serious environmental problems. Therefore, it is necessary to pursue a replacement which can provide an enough protection against corrosion.

In recent years, the hybrid organic–inorganic sol–gel coatings are reported as promising environmentally friendly alternatives for anti-corrosion pre-treatments for different metal substrates due to its outstanding adhesion on metal surface and excellent anti-corrosion performance [3–7]. The hybrid coatings have been applied as protective layers to various metallic substrates, including steel [8, 9], magnesium alloys [10], aluminum alloys [11–13] and copper [14, 15]. In this context, the incorporation of corrosion inhibitors [16–19, 22] and nanoparticles [20–22] into hybrid films has been extensively investigated. However, it suffered from limited effectiveness since the incorporation of cerium ions into the hybrid structures can generate high porosity and lose anti-corrosion ability for a relatively long immersion time [12, 23, 24]. Furthermore, because of capillary force and solvent evaporation stress, some defects, cracks, pores and low binding force will be formed within the hybrid film during the heat-treatment process, which may affect the performance of the hybrid coatings in corrosion protection.

On the other hand, it is well-known that the organic components have good ductility and can facilitate the stress relaxation in the inorganic networks, resulting in a drastic increase in thickness without the cracking or debonding of coatings. A variety of novel sol–gel siloxane-co-polymer hybrids has been applied in anti-corrosion coatings of metallic surfaces [22, 25–29]. Sarmento et al. [27] have presented an investigation of polysiloxane hybrid films based on tetraethoxysilane (TEOS), 3-methacryloxypropyltrimethoxysilane (MPTS) and methyl methacrylate (MMA) on stainless tinplate substrates, exhibiting better corrosion protection for the stainless tinplate samples. However, the barrier effect of the hybrid coatings, indeed, is not very satisfactory due to the low cross-linking density of the silane molecules. Recently, for the corrosion protection of aluminum alloys, Rosero-Navarro et al. [29] have illustrated the incorporation of silica nanoparticles into a hybrid organic–inorganic sol–gel coating, which was constructed from TEOS, 3-metacryloxypropyltrimethoxysilane (MPTS) and ethyleneglycol dimethacrylate (EGDMA). It was found that the addition of EGDMA can lead to a higher cross-linking network and a better corrosion resistance to the aluminum alloy. However, phase separation and subsequent delamination can cause failure of long-term anti-corrosion.

In this contribution, we use triallyl isocyanurate (TAIC), having three C=C double bonds, as a functional monomer, to provide a high degree of cross-linking between organic and inorganic networks by the formation of hybrid coatings at molecular level. Hybrid coatings were synthesized by the acid-catalyzed hydrolytic co-polycondensation of TEOS and 3-metacryloxypropyltrimethoxysilane (MPTS), followed with radical polymerization of MMA and TAIC. The anti-corrosion performances of the hybrid coatings deposited on tinplate were also studied.

2 Experimental procedure

All chemicals used were commercially available. 3-Methacryloxypropyltrimethoxysilane (MPTS, Aldrich, 98 %) and tetraethoxysilane (TEOS, Aldrich, 98 %) were used as received. Triallyl isocyanurate (TAIC, 98 %) and methyl methacrylate (MMA, 98 %) were obtained from Acros Organics. Benzoyl peroxide (BPO, Reagen, 98 %) was used as the initiator, and it was re-crystallized in ethanol solution before use. Absolute ethanol, acetone, hydrochloric acid was purchased from Aladdin Company (Shanghai, China). Deionized water was used through the experiments.

2.1 Preparation of the hybrid coatings

The hybrid coatings were prepared by the sol–gel method in two successive steps. Firstly, MPTS and TEOS were hydrolyzed and condensed by catalysis with HCl at a pH value between three and four in absolute ethanol. Upon adding the deionized water within 1 h, the solution was stirred for 3 h at room temperature. Secondly, the obtained sol was diluted with absolute ethanol, and then the temperature was increased to 70 °C. TAIC, MMA and BPO were added within 1.5 h, and the free radical polymerization reaction was carried out for about 8 h under a nitrogen atmosphere. As a result, the homogenous and transparent hybrid coatings were obtained.

The hybrid coatings prepared at the following MPTS/MMA/TAIC molar ratios of 1:1:0.125, 1:1:0.25, 1:1:0.375 and 1:1:0.5, denoted T1, T2, T3 and T4, respectively. The molar ratio of BPO to C=C groups was controlled at 0.01. The other optimized molar ratios were kept constant: MPTS/TEOS = 1.0, ethanol/Si = 4.0, H_2O/Si = 3.0.

2.2 Surface pretreatment and coating method

Tinplates (150 mm × 70 mm × 3 mm) were used as the substrates, which were polished by metallographic sand paper (1,200 mesh), and degreased with acetone and finally dried at 60 °C for 2 h. The hybrid film was obtained by dip-coating at a withdrawal rate of 15 cm/min. The coated substrates were heated at 110 °C for 2 h and then cooled at a rate of 20 °C/h in order to ensure densification of the gel network.

As shown in Fig. 1, the hybrid coatings have been produced by a sol–gel process consisting of two successive stages. The first step is the formation of the linear sol with methacryloxy functional groups by hydrolysis and condensation of MPTS and TEOS (see Fig. 1a). In the second step, the methacryloxy functional sol, MMA and TAIC with three C=C double bonds are cross-linked through a radical polymerization reaction and therefore interpenetrating network hybrid coatings were obtained (see Fig. 1b). Aging would result in further condensation reaction and the formation of Si–O–Si three-dimensional network, which would improve the corrosion resistance of the hybrid coatings on tinplate. Silanols (Si–OH) is spontaneously adsorbed onto the metal surface through strong van der Waals bonds between the polymer molecules and the metallic surface, forming stable covalent Fe–O–Si bonds during the heat-treatment process (see Fig. 1c).

2.3 Characterization methods

Fourier-transform infrared (FT-IR) spectra were recorded on a Nicolet 370 FT-IR spectrometer using pressed KBr pellets. The hybrid coatings were dried at 110 °C for 2 h and then grinded into powders and the powders were extracted with acetone for 5 h.

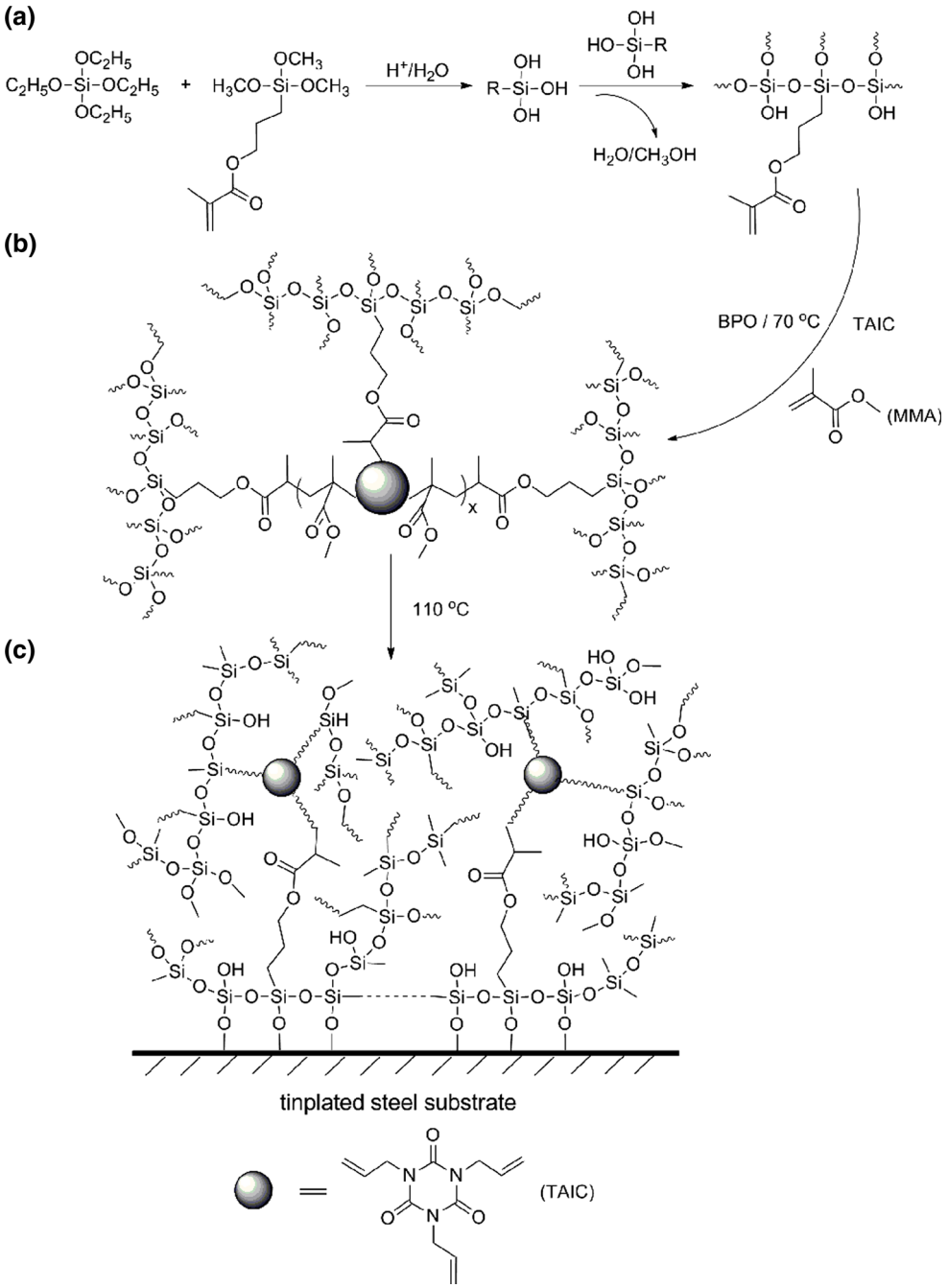

Fig. 1 Reaction scheme of the formation of hybrid coatings: **a** hydrolysis and condensation of TEOS and MPTS; **b** cross-linking reaction; **c** the bonding mechanism between silane molecules and metal substrate

To characterize the surface morphologies of hybrid films, scanning electron microscope (SEM) (SUPRA55, ZEISS, Germany) images were taken using a field-emission SEM operated at an accelerating voltage of 5 kV.

The aqueous contact angle analysis was carried out to determine the wettability of the sol–gel coatings using a Dataphysics OCA 20 with sessile drop method. A 3 μL drop of distilled water was put on the surface with a micro liter syringe and observed with an optical microscope. The value of the contact angle was an average of at least three readings at different locations on the surface of each sample.

To evaluate the thermal behavior of the hybrid coatings, thermo gravimetric analysis (TGA) was performed using a NETZSCH STA 409 C model thermo gravimetric analyzer. About 5 mg samples of the hybrid coatings were placed into the platinum crucibles, and heated at a rate of 10 °C/min up to 650 °C under a nitrogen atmosphere.

The polarization experiments and the electrochemical impedance spectroscopy (EIS) were carried out using a commercial electrochemical workstation (PGSTAT 302, Autolab) in a 3.5 wt% NaCl solution. A conventional three-electrode cell was used in which saturated calomel electrode (SCE) as the reference, a platinum wire as the counter and the

test coupons as the working electrode, respectively. Potentiodynamic tests were conducted at a scan rate of 0.01 V/s after 4 h of immersion. EIS measurements were examined at open circuit potential (OCP) with 10 mV perturbation in the frequency range of 10^5–10^{-2} Hz. Three replications were performed to ensure repeatability.

Corrosion resistance of the coated samples was examined by a neutral salt spray test (SST) according to GB/T 1771-2007. Test was conducted at 35 °C and 0.1 MPa with 5 wt% NaCl solution.

3 Results and discussion

3.1 Structural analysis

The structures of the hybrid coatings were characterized by FT-IR spectra. As shown in Fig. 2, the absorption band at 3,454 cm^{-1} corresponds to the O–H stretching vibration of both water and silanol groups [30–33]. The absorption bands at 2,960 and 2,891 cm^{-1} can be assigned to the asymmetric and symmetric stretching vibrations of the C–H bonds, respectively. There are two carbonyl stretches on the spectra. The band centered at 1,723 cm^{-1} is associated with the symmetric (C=O) stretching vibration in acrylate moiety while the other one centered at 1,697 cm^{-1} is associated to the amide carbonyl groups from TAIC [34]. And absorbance bond at 1,467 cm^{-1} attributed to $–CH_2–$ bending from MMA, MPTS and TAIC. The strong and broad band centered at 1,147 cm^{-1} is probably due to the Si–O–Si, suggesting that the Si–O–Si bearing three-dimensional network has been constructed [31, 32]. IR bands at 3,791 cm^{-1} appear because of the alcoholic OH from the aqueous solution. It is also observed the peak of C=C double bond at 1,636 cm^{-1} is weaker than the original, indicating that TAIC and MMA are cross-linked with the MPTS/TEOS coating to enhance the density of the hybrid coating film. Figure 1 simply describes the hydrolysis and condensation reaction of TEOS and MPTS and the cross-linking reaction for the methacryloxy functional sol with TAIC and MMA.

3.2 Thermal analysis

The polymerization of the organic moieties was confirmed by the TGA curves and the differential weight loss (DTG) of the powder samples, as shown in Fig. 3. The weight loss at 0–200 °C corresponds to the evaporation of non-bonded water and other volatile compounds. The DTG of MPTS/TEOS coating has two degradation stages. The first degradation stage above 414 °C was ascribed to the random scission within the polymer chain [35]. The weak degradation event above 473 °C can be attributed to the dehydration of silanol groups in the SiO_2 network [35]. It should be noted that the hybrid coatings (T1, T2, T3, T4) show higher thermal stability of about 444, 460, 459 and 460 °C, respectively, compared with that of MPTS/TEOS coating. Obviously, the enhancement in the thermal stability of the copolymers increases with the increasing TAIC content, which may be related to the stability isotriazine ring of TAIC and the interpenetrating network of hybrid coatings.

3.3 Scanning electron microscopy analysis

As shown in Fig. 4a, relatively wide cracks appear on the MPTS/TEOS coating. These cracks are presumably formed during the dry process as the result of strong capillary forces [36]. As illustrated in Fig. 4b–d, it is obvious that the morphologies of the hybrid coatings are free of crack and highly homogeneous. These results can be attributed to the fact that the hybrid films showed a good interaction interface between the silica particles and the organic polymer. Though some

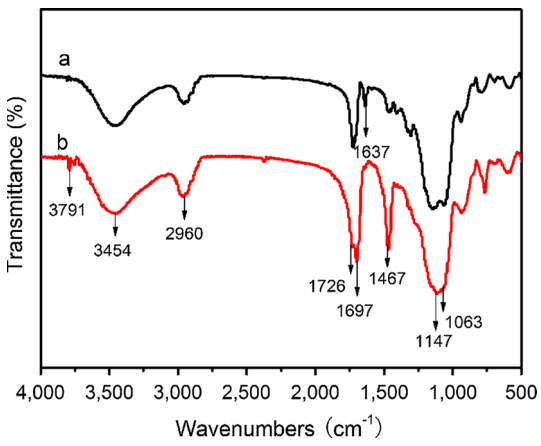

Fig. 2 FT-IR spectra of MPTS/TEOS coating (**a**) and the hybrid coating (**b**)

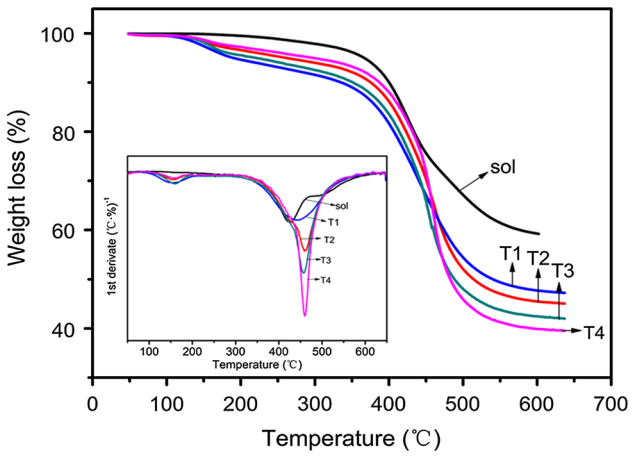

Fig. 3 TGA and DTG (*insert*) curves of the MPTS/TEOS coating and the hybrid coatings with different TAIC content

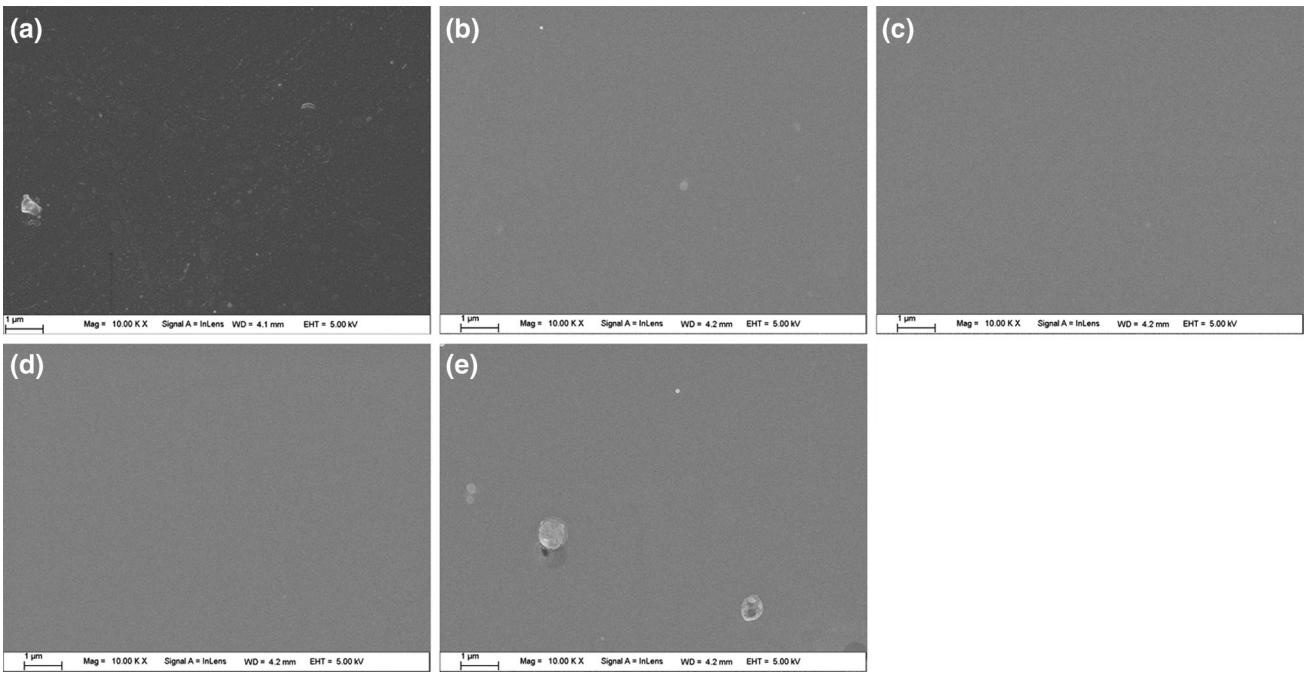

Fig. 4 Surface morphologies of the hybrid coatings covered tinplate substrate **a** sol, **b** T1, **c** T2, **d** T3, **e** T4

pores can still be seen on the surface of T4 hybrid coating (see Fig. 4e), the surface is very smooth. The higher degree organic polymerized sols usually present a higher density of defects, and the pores and micro-cracks obtained coatings present a lower protection behavior [29].

3.4 Surface wettability

Water static contact angle is an important parameter reflecting the wetting characteristics of the tinplate and the coating surface. The hydrophobic properties of the sol gel coatings are examined by the contact angle measurements. Water has been used as a test liquid to establish whether a coating is hydrophilic (angle <45°), hydrophobic (angle >90°) or somewhere in between (angle of 45–90°). Water contact angle data were measured to determine the wettability properties of the bare and coated tinplate surface. The images of water droplet on the tinplate surfaces are shown in Fig. 5. In Fig. 5a, water contact angle is 24° on the bare tinplate surface. The contact angles of MPTS/TEOS coating is 63°, while in the cases of T1-4 are 64°, 62°, 64°, and 63°, respectively. It means that the addition of TAIC and MMA does not remarkably change the wetting characteristics of MPTS/TEOS coating.

3.5 Corrosion analysis

3.5.1 Polarization curves

Figure 6 shows that the polarization curves were recorded for the bare tinplate and the hybrid coatings coated after 4 h of immersion in neutral 3.5 wt% NaCl solution. From these experiments, some important parameters such as corrosion current density, and corrosion potential can be determined by the Tafel curve [37], and the results are listed in Table 1. In addition, the protection efficiencies were calculated according to the equation [38]:

$$\eta = \left(1 - \frac{\text{icorr}}{\text{i°corr}}\right) \times 100\,\%$$

where $i°_{corr}$ and i_{corr} are the corrosion current density of bare tinplate and the corrosion current density of tinplate coated with hybrid coatings, respectively. The values of protection efficiency η are also listed in Table 1.

In Fig. 6 and Table 1, the corrosion potentials of MPTS/TEOS, T1, T2, T3 and T4 are −757, −703, −772, −649 and −695 mV, respectively, and the corrosion potential of the bare sample is −937 mV. The corrosion potential of the hybrid coatings are not largely different from the MPTS/TEOS coating, indicating the hybrid coatings provide a similar protection. As shown in Table 1, the current density is increased in such an order: T3 < T2 < T4 < T1 < MPTS/TEOS < bare tinplate. The values of the protection efficiency of MPTS/TEOS, T1, T2, T3 and T4 are calculated by Eq. (1) to be 70.01, 94.13, 99.39, 99.96 and 99.06 %, respectively. These findings indicate an obvious decrease in the corrosion rate of the coated samples compared with the bare tinplate, suggesting an effective protection of tinplate surface by the hybrid coatings. As compared to the bare tinplate (7.455×10^{-5} A cm^{-2}), the i_{corr} value for T3 hybrid coating (2.727×10^{-8} A cm^{-2}) is greatly reduced by three orders in

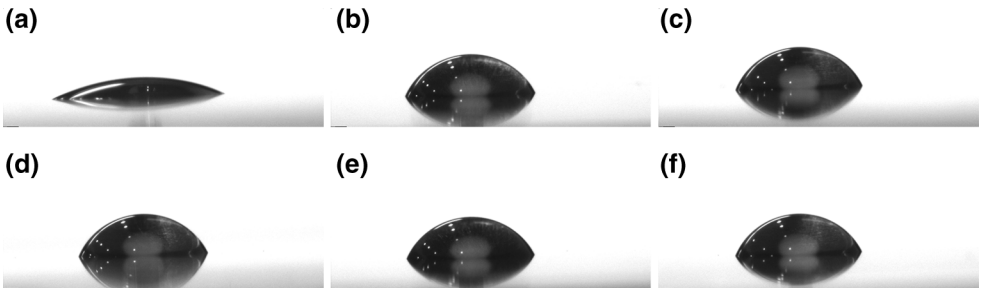

Fig. 5 Photos of water droplet on tinplate surfaces: **a** bare tinplate, **b** sol, **c** T1, **d** T2, **e** T3, **f** T4

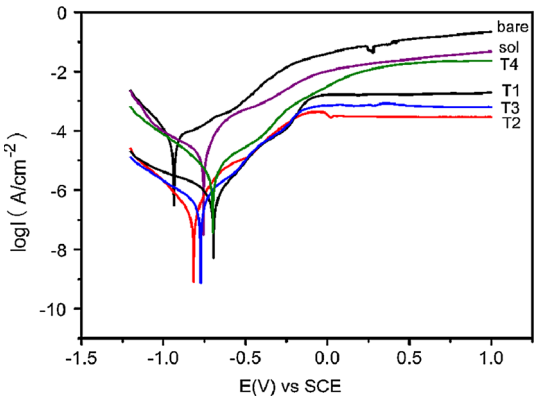

Fig. 6 Polarization curves of bare tinplate, MPTS/TEOS coating, and T1, T2, T3, T4 in 3.5 wt% NaCl solution

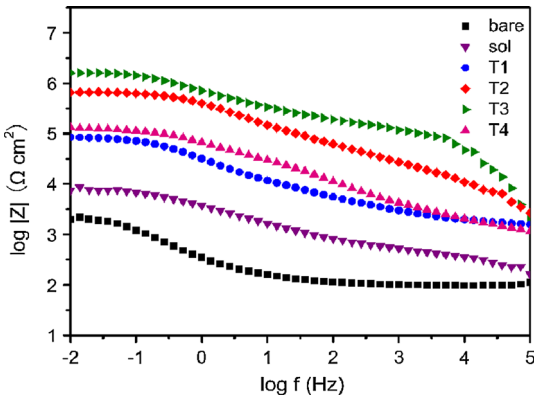

Fig. 7 Bode polts representation of EIS results for bare tinplate and hybrid coatings covered tinplate electrodes after 4 h immersion in 3.5 wt% NaCl solution

Table 1 Electrochemical parameters for the bare tinplate and hybrid coatings covered tinplate electrode obtained from the polarization curves and EIS measurements

Electrode	E_{corr}/mv (vs SCE)	I_{corr}/A cm^{-2}	η (%)	$\|Z\|_{0.01}$ (Ω cm^2)
Bare	937	7.455×10^{-5}	–	1.91×10^3
sol	757	2.236×10^{-5}	70.01	7.76×10^3
T1	703	4.374×10^{-6}	94.13	8.51×10^4
T2	772	4.537×10^{-7}	99.39	6.61×10^5
T3	649	2.727×10^{-8}	99.96	1.55×10^6
T4	695	7.024×10^{-7}	99.06	1.29×10^5

magnitude. The increase of the TAIC content tends to promote the formation of higher cross-linked, dense film with better corrosion resistance due to the addition of cross-linking agent. However, an excess of TAIC content (T4 hybrid coating) could produce some defects such as pores and particles as shown in Fig. 4e, and during the aging of the coating, the particle would further increase by continuous hydrolysis and condensation. The existence of pores and particles will destroy the integrity of films. So, it can be concluded that the hybrid coatings provide excellent corrosion protection to the tinplate substrate by forming a good physical barrier, which effectively prevent O_2, H_2O and Cl^- from reaching the tinplate surface.

3.5.2 *Electrochemical impedance*

Figure 7 shows the EIS results for coated tinplate electrodes along with the bare tinplated electrode after 4 h of immersion in 3.5 wt% NaCl solution. The values of impedance modulus ($|Z|_{0.01}$) at 0.01 Hz are listed in Table 1, giving a sequence of T3 > T2 > T4 > T1 ≫ MPTS/TEOS > bare tinplate. It can be found that the $|Z|_{0.01}$ values of coated samples are higher than that of the bare tinplate, indicating the corrosion rate at the coated samples is lower than that at the bare one. For T3, the value of $|Z|_{0.01}$ (1.55×10^6 Ω cm^2) is greatly increased by three orders in magnitude compared to the MPTS/TEOS sample (7.76×10^3 Ω cm^2). These results indicated that the TAIC can significantly enhance the protection performance of the MPTS/TEOS coating, which agrees well with the polarization curves.

3.5.3 *Neutral salt spray test*

Salt spray test is often used to evaluate the corrosion resistance performance of the metal substrates. Figure 8

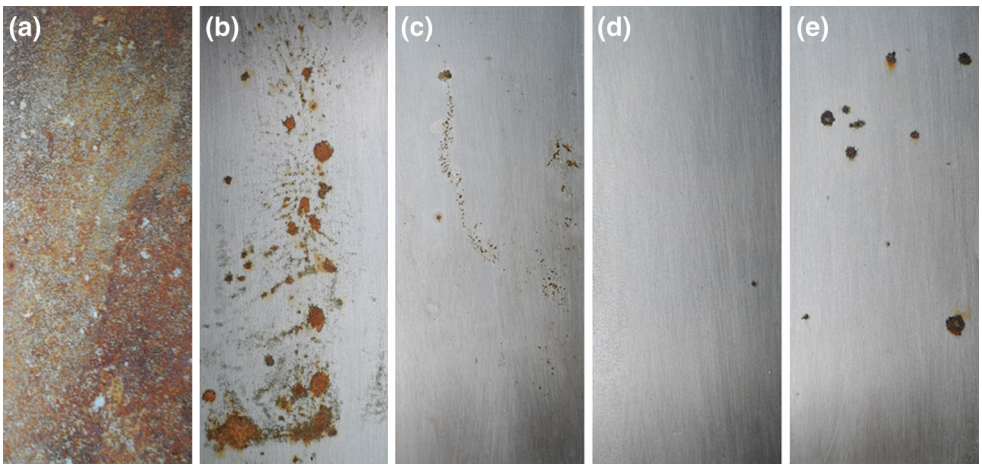

Fig. 8 Photograph of sate spray test after different exposure times: **a** bare tinplate, **b** MPTS/TEOS coating, **c** T1, **d** T2, **e** T3, **f** T4

shows the photographs of the coated tinplate and the bare tinplate after exposure to neutral salt spray for different time. For the coated MPTS/TEOS coating, corrosion was visible to the naked eye after exposure for 96 h (see Fig. 8a). As depicted in Fig. 8b–e, the hybrid coatings show very good resistance to salt spray than the MPTS/TEOS coating. Notably for T3, no obvious corrosion occurs on the tinplate surface after being exposed in salt spray for 200 h (see Fig. 8d). Pitting corrosion occurs on the tinplate coated with T2 hybrid coating (see Fig. 8c). These favorable results suggest that the hybrid coatings provide an excellent salt spray resistance for the tinplate than the MPTS/TEOS coating. However, the T4 hybrid coating provides a poor corrosion protection compared with the T3 hybrid coating (see Fig. 8e), which can be observed from the surface morphologies of the T4 hybrid coating.

The salt spray results coincided with the polarization curves and the impedance spectra, implying that the hybrid coatings can effectively improve the corrosion performance via increasing barrier properties of the MPTS/TEOS coating. Excellent anti-corrosion performances of the hybrid coatings for tinplate can be attributed to the fact that TAIC and MMA play synergetic roles in the enhancement of sol corrosion resistance: (1) TAIC acts as a tri-functional cross-linking reagent and it can make methacryloxy functionalized sol–gel coating denser to improve the physical barrier effect of coatings; and (2) MMA functions as an organic monomer and it improves a good corrosion resistance in the hybrid coatings.

4 Conclusions

A more compact dense and crack free hybrid inorganic–organic coating with interpenetrating network doped layer was developed to improve the anti-corrosion ability of tinplate. The results of potentiodynamic polarization, EIS and SST show that the hybrid coatings can significantly improve the corrosion protection for tinplate. Higher impedance value and lower current density were observed for the tinplate coated with the hybrid coatings. The thermal stability of the hybrid coatings (460 °C) is also higher than that of the MPTS/TEOS coating (414 °C).

Acknowledgments The authors thank Yong Kong and Sheng-Chun Chen for their useful comments about the linguistic content of the article.

References

1. Bhattacharyya S, Das MB, Sarkar S (2008) Eng Fail Anal 15:711–722
2. McCafferty E (1989) Corros Sci 29:377–391
3. Zheludkevich ML, Ferreira MGS, Salvado IM (2005) J Mater Chem 15:5099–5111
4. Seifzadeh D, Golmoghani-Ebrahimi E (2012) Surf Coat Technol 210:103–112
5. Osborne JH, Blohowiak KY, Taylor SR, Hunter C, Bierwagon G, Carlson B, Bernard D, Donley MS (2001) Prog Org Coat 41:217–225
6. Zheng XS, Li JH (2010) J Sol Gel Sci Technol 54:174–187
7. Wang H, Akid R, Gobara M (2010) Corros Sci 52:2565–2570
8. Gallardo J, Duran A, de Damborenea JJ (2004) Corros Sci 46:795–806
9. Chou TP, Chandrasekaran C, Limmer SJ, Seraji S, Wu Y, Forbess MJ, Nguyen C, Cao GZ (2001) J Non-Cryst Solids 290:153–162
10. Supplit R, Koch T, Schubert U (2007) Corros Sci 49:3015–3023
11. Wittmar A, Wittmar M, Ulrich A, Caparrotti H, Veith M (2012) J Sol Gel Sci Technol 61:600–612
12. Zheludkevich ML, Serra R, Montemor MF, Miranda Salvado IM, Ferreira MGS (2006) Surf Coat Technol 200:3084–3094
13. Moutarlier V, Neveu B, Gigandet MP (2008) Surf Coat Technol 202:2052–2058
14. Tan ALK, Soutar AM (2008) Thin Solid Films 516:5706–5709
15. Peng S, Zhao W, Li H, Zeng Z, Xue Q, Wu X (2013) Appl Surf Sci 276:284–290

16. Moutarlier V, Neveu B, Gidandet MP (2007) Surf Coat Technol 202:2052–2058
17. Khramov AN, Voevodin NN, Balbyshev VN, Mantz RA (2005) Thin Solid Films 483:191–196
18. Raps D, Hack T, Wehr J, Zheludkevich ML, Bastos AC, Ferreira MGS, Nuyken O (2009) Corros Sci 51:1012–1021
19. Tamar Y, Mandler D (2008) Electrochim Acta 53:5118–5127
20. Rosero-Navarro NC, Pellice SA, Castro Y, Aparicio M, Durán A (2009) Surf Coat Technol 203:1897–1903
21. Rajath Varma PC, Colreavy J, Cassidy J, Oubaha M, Duffy B, McDonagh C (2009) Prog Org Coat 66:406–411
22. Palomino LM, Suegama PH, Aoki IV, Montemor MF, Melo HG (2008) Corros Sci 50:1258–1266
23. Liu Y, Sun D, You H, Chung JS (2005) Appl Surf Sci 246:82–89
24. Rosero-Navarro NC, Pellice SA, Durán A, Ceré S, Aparicio M (2009) J Sol Gel Sci Technol 52:31–40
25. Hammer P, dos Santos FC, Cerrutti BM, Pulcinelli SH, Santilli CV (2012) J Sol Gel Sci Technol 63:266–274
26. Yu Q, Xu J, Han Y (2011) Appl Surf Sci 258:1412–1416
27. Sarmento VHV, Schiavetto MG, Hammer P, Benedetti AV, Fugivara CS, Suegama PH, Pulcinelli SH, Santilli CV (2010) Surf Coat Technol 204:2689–2701
28. Sakai RT, da Cruz FMD, de Meloc HG, Benedettib AV, Santillib CV, Suegama PH (2012) Prog Org Coat 74:288–301
29. Rosero-Navarro NC, Pellice SA, Castro Y, Aparicio M, Durán A (2009) Surf Coat Technol 203:1897–1903
30. Franquet A, Terryn H, Vereecken J (2003) Thin Solid Films 441:76–84
31. Aguiar H, Serra J, González P, León BJ (2009) J Non-Cryst Solids 355:475–480
32. Li YS, Ba A (2008) Spectrochimica Acta Part A 70:1013–1019
33. Finocchio E, Macis E, Raiteri R, Busca G (2007) Langmuir 23:2505–2509
34. Li R, Zhao R, Zhang H, Li C, Feng D, Qin P, Tan T (2010) Chromatographia 72:47–54
35. Kashiwagi T, Morgan AB, Antonucci JM, VanLandingham MR, Harris RH, Awad WH, Shields JR (2003) J Appl Polym Sci 89:2072–2078
36. Tamar Y, Mandler D (2008) Electrochim Acta 53:5118
37. Weng CJ, Chang CH, Peng CW, Chen SW, Yeh JM, Hu CL, Wei Y (2011) Chem Mater 23:2075–2083
38. Hausler RH (1977) Corrosion 33:117–122